ECCOMAS Congress 2016
VII European Congress on Computational Methods in Applied Sciences and Engineering
M. Papadrakakis, V. Papadopoulos, G. Stefanou, V. Plevris (eds.)
Crete Island, Greece, 5–10 June 2016

FRACTURE OF THIN METAL SHEETS WITH DISTRIBUTION OF GRAIN SIZES IN THE LAYERS

Natalia V. Skripnyak[1,2], Vladimir V. Skripnyak[1], Vladimir A. Skripnyak[1,3]

[1] National Research Tomsk State University
36 Lenin Avenue, 634050 Tomsk, Russia
e-mail: skrp@ftf.tsu.ru

[2]Linköping University
Linköping, SE-581 83 Sweden.
e-mail: natali.skrp@mail.ru

[3]Institute of Strength Physics and Materials Sciences SB RAS
2/4, pr. Akademicheskii, Tomsk, 634021, Russia
e-mail: skrp2006@yandex.ru

Keywords: Multi-scale Simulation, Shock Waves, Grain Size Distribution, Light Alloys, Mechanical Behaviour.

Abstract. *The influence of ultra-fine grained surface layers on the fracture of light alloys sheets was studied by the method of multiscale simulation. The deformation and damaging of 3D structured elementary volumes of thin metal sheets with structured surface layers under tension and compression were calculated. The modified smooth particle hydrodynamics method was used for numerical simulation. It was found that inelastic deformation and the damage are localized at the boundary between ultrafine-grained and coarse grained layers. The deflection of cracks caused by the residual stresses lead to ductility increasing of metal sheets with layered ultrafine-grained and coarse-grained structure. Fracture of thin sheets of aluminium, magnesium and titanium alloys with nanostructured and fine grained surface layers under loading has probabilistic character and depends on parameters of layered structure.*

1 INTRODUCTION

Metallic multilayered structures can be created in thin metal sheets using a technology of surface severe plastic deformation (S^2PD) such as accumulative roll bonding (ARB) [1], ultrasonic shot peening (USSP) [2], surface severe plastic deformation under friction (SPDF) [3], surface mechanical grinding treatment (SMGT) [4], high-energy shot peening (HESP) [5,6], surface mechanical attrition treatment (SMAT) [7].

Metallic multilayers structures exhibit a very pronounced size effect where the mechanical strength depends on the layer thickness. Using S^2PD nanocrystalline layers in the surface of various materials, such as alloys with a face centered cubic (FCC) structure (Al alloy [1-3]), alloys with a hexagonal close-packed HCP structure (magnesium and alpha-titanium alloys [4-13]), and alloys with a body centered cubic (BCC) structure (stainless steel [7]) have been successfully produced.

In recent years, the microstructures and properties of surface layer were systematically investigated in various S^2PD metals and alloys, including BCC, FCC and HCP crystal structures [14].

It was found that as a result S^2PD on the surface of the bulky body are formed with surface layers of NC and UFG structures [1-14].

The fields of residual stresses are formed in the surface layers of bodies [15-17]. The magnitude and sign of residual stress change with increasing distance from the surface.

Generally, compressive stresses reach their maximum at distances ~50-60 μm from the surface. Compressive residual stresses decrease with increase in distance from the surface and change the sign.

Authors [2-10] have shown that compressive stresses in plates subjected to S^2PD operate in the near-surface layer with a thickness of 200-500 μm. Distribution of grain sizes in the layers and residual stresses in thin metal sheets influences on the strength, the fatigue strength and the strain to fracture [18-19].

Guo and co-workers [7] have shown that nanograined interface layer (NGIL) can enhance the ductility of the co-rolled surface mechanical attrition treatment (SMAT) 304 stainless steel (SS), but the ductility will not increase if the NGIL thickness goes beyond 60 μm.

Liu and co-workers [5] have shown that the nanostructured surface layers can be created by using a high-energy shot peening on the low carbon steel. The average grain size in the surface layer can be as small as tens of nanometers, and gradually increases with the distance from the surface.

The yield strength was found to be significantly enhanced without considerable degradation in the ductility and the toughness. Yang and coworkers [6] have shown that rolling or shot-peening of titanium alloys induces growth of the residual stress at the surface layers. Stress concentrations grow at the interface between ultrafine-grained (UFG), nano-grained (NG) and coarse-grained (CG) layers with increasing deformation.

Results of researches testify that reduction in the size of grain of aluminum, magnesium, and titanium alloys causes enhanced strength and ductility under quasi-static loading conditions [18,19]. It was revealed that grains of nanostructured (NS) and ultrafine-grained (UFG) alloys have size distributions. The yield strength and strength under compression and tension, elongation to fracture of light alloys depends on the grain size distribution.

Features of deformation and fracture of thin metal sheets after treated by with S^2PD are defined by shear bands formation, nucleation and growth of damages, coalescence damages under formation of mesoscale and macroscale cracks.

Mechanisms of fracture of light metal sheets with distribution of grain sizes in the surface layers are poorly investigated. We present computational model and results of numerical simulation of damaging and fracture of aluminium and magnesium thin sheets with distribution of grain sizes in the surface layers under dynamic loading.

2 CONSTITUTIVE MODEL

The multilevel computer simulation method was used for numerical research on damage and fracture of thin sheet of aluminium, magnesium, titanium alloys with NGIL and UFG layers [20, 21]. Figure 1.a shows the variation of grain size with depth of surface layer of aluminum alloy 7075 after USSP [2].

Model layered structure thin metal sheet was created using the experimental data on grains structures.

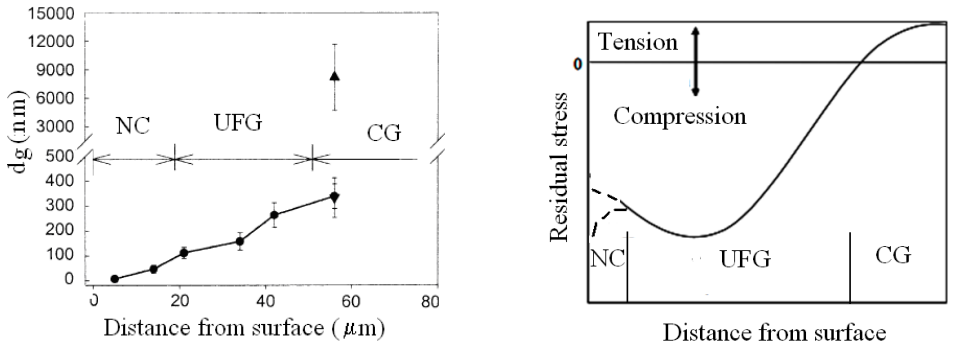

a b

Figure 1. (a) Grain size in the surface layer of aluminum alloy 7075 after USSP. (b) Model residual stress in metal sheet after S^2PD.

Mechanical behavior of thin metal sheet with distribution of grain sizes in the surface layer was simulated under axial tension and compression at high strain rates. 3D model of the elementary volume was used for simulation of deformation and damage. The 3-D volume dimension of 1000 x 100 x 100 μm includes nanocrystalline and ultra-fine grained volumes of surface layers, coarse grained volume with a residual stress.

In the model, the second volume of the surface layer, which is formed in alloys of aluminum, magnesium and titanium as a result of S^2PD was considered. This layer is limited to the surfaces S_3 and S_4. The second layer has a thickness of ~ 100−200 μm and composed of grains having an unimodal or bimodal distribution of grain size. In this work it was assumed that the size distribution of grains is the unimodal with an average size of ~ 800 nm. The second layer is limited to the surfaces S_4 and S_5.

Figure 1.b shows the characteristic change of the residual stresses near the surface of metal alloys after SMAT [15,16]. The surface S_6 in the model correspond to the boundary on which the residual stresses close to zero. It was assumed that S_6 is at a distance of ~350 μm from the plate surface.

Mechanical behavior of structured volume is described using the approach to damaged elastic-plastic medium [15]. Smooth particles hydrodynamic (SPH) method was used for the numerical simulation [22].

The scheme of boundary conditions is shown in Fig. 2.

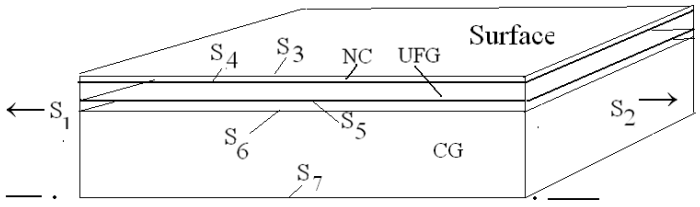

Figure 2. Boundary conditions.

The boundary conditions were written in the form:

$$u_k(x_k,t)=u_k(x_k,t),\ x_k \in S_1, x_k \in S_2,\ \sigma_{ij}(x_k,t)=0, x_k \in S_3\ . \quad (1)$$

where u_k are components of particle velocity vector, t is time, x_k are Cartesian coordinates.

It was assumed that there is no slip between the layers of the grain structure.

Initial condition describes the distribution of the residual stress and the residual strain:

$$u_k(x_k,0)=0;\ T(x_k,0)=T_0, x_k\in\Omega;\ \sigma_{kk}(x_k,0)=\sigma_R(x_k,0);\varepsilon_{kk}(x_k,0)=\varepsilon_R(x_k,0); x_k\in\Omega_{S_3\cup S_6}, \quad (2)$$

where Ω is the elementary volume, $\Omega_{S_3\cup S_6}$ is the volume in which there are residual stresses.

Kinematics of medium was described by the local strain rate tensor:

$$\dot{\varepsilon}_{ij}=\frac{1}{2}(\nabla_i u_j+\nabla_j u_i)\ , \quad (3)$$

where $\dot{\varepsilon}_{ij}$ are components of the strain rate tensor, u_i are components of particles velocity vector, ∇_i is Hamilton operator.

Components of strain rate tensor are expressed by sum of elastic and inelastic terms:

$$\dot{\varepsilon}_{ij}=\dot{\varepsilon}^e_{ij}+\dot{\varepsilon}^n_{ij}\ , \quad (4)$$

where $\dot{\varepsilon}^e_{ij}$ are components of the elastic strain rate tensor, $\dot{\varepsilon}^n_{ij}$ are components of the inelastic strain rate tensor.

Dynamics of volume is described in Lagrange coordinate system by mass conservation, momentum conservation and energy conservation equations:

$$\frac{\partial\sigma_{ij}}{\partial x_j}=\rho\frac{du_i}{dt},\ \frac{d\rho}{dt}=\rho\frac{\partial u_i}{\partial x_i},\ \rho\frac{dE}{dt}=\sigma_{ij}\dot{\varepsilon}_{ij}, \quad (5)$$

where σ_{ij} are components of stress tensor, ρ is the mass density, u_i are components of particles velocity vector, ε_{ij} is components of strain rate tensor, E is the specific internal energy per unit mass.

The bulk inelastic strain rate is described by relation:

$$\dot{\varepsilon}^n_{kk}=\frac{1}{3}\frac{\dot{D}}{(1-D)}\ , \quad (6)$$

where D is the damage parameter, the substantial time derivative is denoted via dot notation.

Damage accumulation during inelastic deformation of UFG metals leads to limited ductility of metal sheet with hardened surface layers. The local damage parameter D is introduced in the form:

$$D=\int_0^{t_f}\frac{\dot{\varepsilon}^n_{eq}}{\varepsilon^n_f}dt \quad (7)$$

where $\dot{\varepsilon}^n_{eq}=(\frac{2}{3}\dot{\varepsilon}^n_{ij}\dot{\varepsilon}^n_{ij})^{1/2}$, ε^n_f is the threshold of inelastic strain, t_f.is the time before local fracture.

For material particle the local failure criterion is written in the form:

$$D = 1. \quad (8)$$

When using SPH, numerical method criterion (8) determines the loss in strength of the damaged material in the particle [20].

Local fracture criterion (8) was used for NC and UFG light alloys at the room and elevated temperatures owing to relatively low melting temperature of light alloys. The melting temperature of aluminum and magnesium alloys is equal to~ 900 K.

Phenomenological relations (9) were used for calculation of the threshold inelastic strain ε^n_f:

$$\varepsilon_f^n \quad (d_g) / \varepsilon_f^{CG} = A_2 + (A_1 + A_2) / (1 + \exp[(x - x_0) / \bar{x}]),$$

$$\varepsilon_f^{CG} \quad = D_1 (P^* + T^*)^{D_2}, \tag{9}$$

where ε_f^{CG} is a strain to fracture for coarse grained material, x corresponds to $d_g^{-1/2}$, A_1, A_2, x_0, $\bar{x}$ are material constants, $T^*=\sigma_{sp}/P_{HEL}$, $P^*=p/P_{HEL}$, P_{HEL} is the pressure corresponding to the Hugoniot Elastic Limit, D_1, D_2 are material constants.

The threshold inelastic strain corresponds to the strain at fracture under quasistatic loading.

Figure 3 shows the dependence of normalized values of the strain at fracture versus the inverse square root of the average grain size.

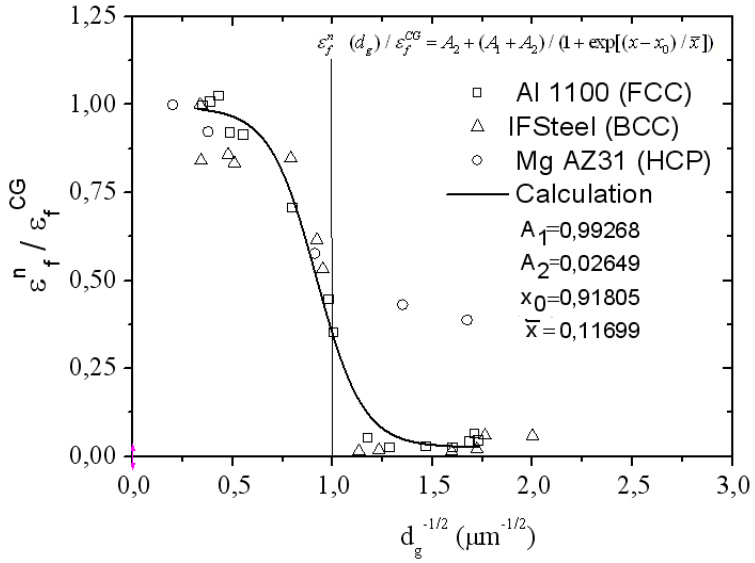

Figure 3. Normalized values of the strain at fracture vs the inverse square root of the average grain size.

The ductility of UFG light alloys increases when a relative part of coarse grains in volume is decreased. The dependence of the strain to fracture on specific volume of coarse grains in UFG Al-Mg alloy with a bimodal grain sizes distribution described by the relation [20,22]:

$$D_1 \ = 0.01 exp(\ C_{cg} / 0.363), \tag{10}$$

where D_1 is the strain to fracture under quasi-static tension, C_{cg} is the specific volume of coarse grain size of light alloys.

The criterion (8) defines a local destruction of material particles. The process of damage and fracture at a higher structural level is considered as the formation of a spatial cluster of damaged particles in an elementary volume. When using the SPH method for the numerical simulation of deformation and fracture of a model volume of plates cracking is described using the spatial formation of clusters of particles with broken bonds with neighbouring particles. The particles belonging to a given cluster is determined by the condition:

$$r_{\alpha\beta} = \sum_{i=1}^{3} (x_i^{\alpha} - x_i^{\beta})^2 > L, \tag{11}$$

where $r_{\alpha\beta}$ is the distance between neighbouring particles α and β, L is the parameter close to the particle sizes, $L > d + \varepsilon_{lim} d$, d is the size of particle, ε_{lim} is the maximum allowable strain at the crack tip.

The pressure is calculated by polynomial equation of state [22]. The stress tensor deviator is calculated by the equation:

$$d\,S^{(m)}_{ij}/d\,t = 2\mu(\dot{e}_{ij} - \dot{e}_{ij}{}^{p}), \tag{12}$$

where d/dt is the Jaumann derivative, μ is the shear modulus, $\dot{e}_{ij} = \varepsilon_{ij} - (1/3)\delta_{ij}\dot{\varepsilon}_{kk}$ is the deviator of the strain rate tensor, and $\dot{e}^{n}_{ij}$ is the deviator of the inelastic strain rate tensor.

The deviator of the inelastic strain rate tensor is written as:

$$\dot{e}^{p}_{ij} = (3/2)[S_{ij}\,\dot{e}^{p}_{eq}/\sigma_{eq}]. \tag{13}$$

$$(3/2)(S_{ij} - R_{ij})(S_{ij} - R_{ij}) = \sigma_s{}^{2}. \tag{14}$$

where $\dot{R}_{ij} = C_r(R_{eq}\,\dot{e}^{p}_{ij} - R_{ij}de^{p}_{eq})$, $\sigma_{eq} = [3/2\,S_{ij}\,S_{ij}]^{1/2}$, $\sigma_{ij} = -p\,\delta_{ij} + S_{ij}$, $\dot{e}^{p}_{eq} = [(2/3)\dot{e}^{n}_{ij}\,\dot{e}^{n}_{ij}]^{1/2}$, $\dot{\varepsilon}^{n}_{ij} = (1/3)\dot{\varepsilon}^{n}_{kk}\delta_{ij} + \dot{e}^{n}_{ij}$, δ_{ij} is the Kronecker delta, C_r is material parameter. C_r varies from 200 to 500 for light alloys.

For FCC, HCP and BCC alloys the yield stress was calculated by the modified Zerilli-Armstrong constitutive model [24,25]:

$$\begin{gathered}
\sigma_s = \sigma_{s0} + [C_6 d_g^{-1/2} + C_5(\varepsilon^{p}_{eq})^{n_1}]\exp[-T\ln(\dot{\varepsilon}_{eq}/\dot{\varepsilon}_a)] + C_1\exp[-C_3T + C_4T\ln(\dot{\varepsilon}_{eq}/\dot{\varepsilon}_b)] \text{ for HCP alloys, or} \\
\sigma_s = \sigma_{s0} + C_6 d_g^{-1/2} + C_2(\varepsilon^{p}_{eq})^{1/2}\exp[-C_3(1 - \ln\dot{\varepsilon}/\ln\dot{\varepsilon}_b)T] + \\
+ C_4[\varepsilon_r(1 - \exp(-\varepsilon_{eq}/\varepsilon_r))]^{1/2}\exp[-TC_7(1 - \ln(\dot{\varepsilon}_{eq}/\ln\dot{\varepsilon}_a))], \\
\sigma_s = \sigma_{s0} + C_6 d_g^{-1/2} + C_5(\varepsilon^{p}_{eq})^{n_1} + C_1\exp[-C_3T + C_4T\ln(\dot{\varepsilon}_{eq}/\dot{\varepsilon}_{eq0})] \text{ for BCC alloys,} \\
\sigma_s = \sigma_{s0} + C_6 d_g^{-1/2} + C_2(\varepsilon^{p}_{eq})^{1/2}\exp[-C_3T + C_4T\ln(\dot{\varepsilon}_{eq}/\dot{\varepsilon}_{eq0})] \text{ for FCC alloys.}
\end{gathered} \tag{15}$$

where C_1, C_2, C_3, C_4, C_5, C_6, C_7, n_1, ε_r , $\dot{\varepsilon}_a$, $\dot{\varepsilon}_b$ are materials parameters, T is the temperature in [K].

Parameter	Al–6% Mg–0.3% Si.		Ma2-1 (AZ31)		Ti6Al4V	
Grain size,[μm]	$1<d_g<100$	$0.1<d_g<1$	$1 < dg<100$	$0.1< dg<1$	$1< dg<100$	$0.1< dg<1$
σ_{s0} ,[MPa]	300	510	80	330	190	570
C_1,[MPa]	52		149			
C_2,[MPa]	99		160		139	
C_3, [K^{-1}]	0.0042		0.0162		0,0024	
C_4, [K^{-1}]	0.00158		0.00178		0,00043	
C_5,[MPa]			570		656	
C_6,[MPa $\mu m^{1/2}$]	326	11	303	180	1200	350
C_7, [K^{-1}]	0		0		0	
n_1	0.179		0.17		0.5	
ε_r					0.1877	
$\dot{\varepsilon}_a$, [s^{-1}]	1,0		1,0		$8{,}25\ 10^5$	
$\dot{\varepsilon}_b$, [s^{-1}]	1,0		1,0		$1.6\ 10^4$	

Table 1. Constitutive parameters for FCC and HCP light alloys.

The yield strength of magnesium and titanium alloys under tension versus $d_g^{-1/2}$ (d_g, average grain size) shown in Figure 4a. The yield strength of aluminium alloys under tension versus $d_g^{-1/2}$ shown in Figure 4b.

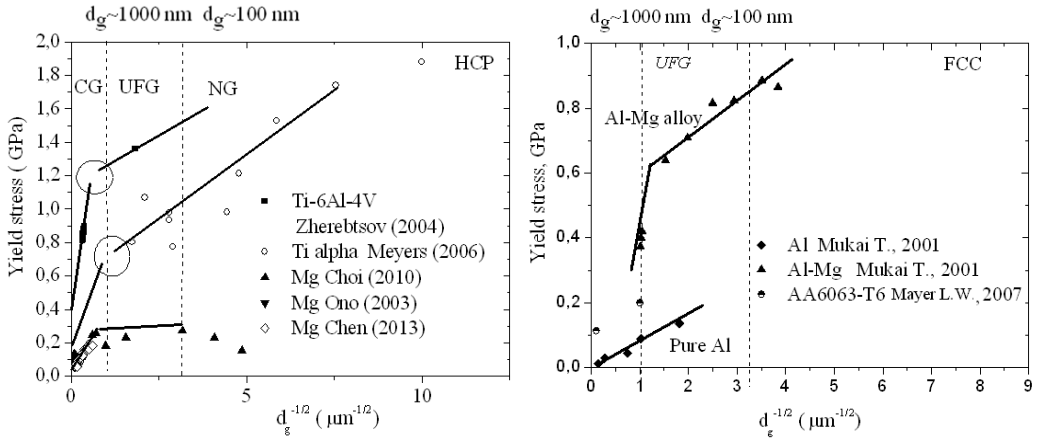

a b

Figure 4. (a) The yield strength of magnesium and titanium alloys versus $d_g^{-1/2}$ (d, average grain size). (b) The yield strength of aluminium alloys versus $d_g^{-1/2}$.

Damage accumulation in sheets of aluminum alloy Al 7075 and magnesium Ma2-1 (this is analog to AZ31 magnesium alloy) with strengthened layers under tension-compression was simulated. Numerical method was discussed in [22].

3 RESULTS AND DISCUSSION

Fig. 5a shows the damage in the section of the model layered aluminium sheet after 50 cycles of uniaxial tension - compression under stress amplitude ~1.02 σ_s. Strain rate was equal to 1 s^{-1}.

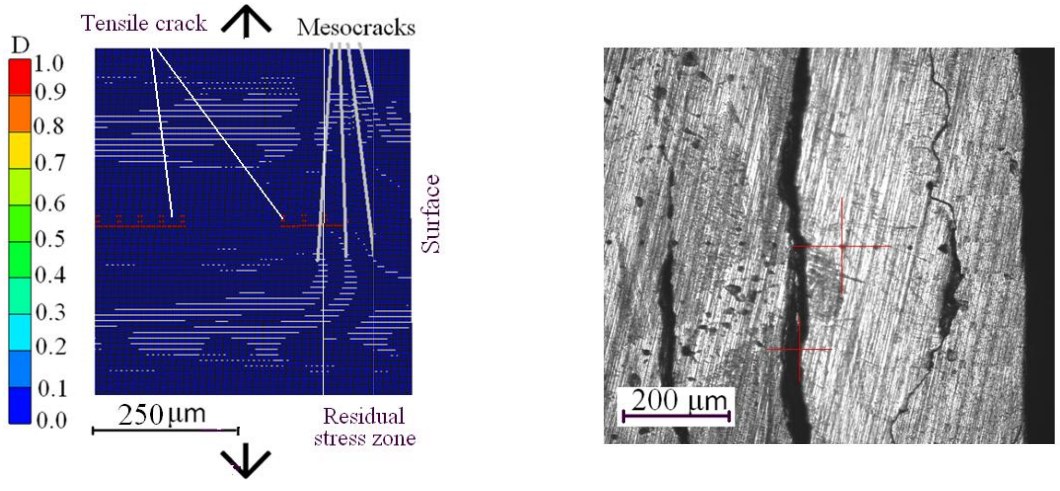

a b

Figure 5. (a) The distribution of calculated values of damage under tension-compression model the volume of a sheet of aluminum alloy with hardened surface layers. (b) Damage in the surface layer of the aluminium alloy sheet with an initial thickness of 1.5 mm after 50 cycles of axial tension-compression.

Under tension damages nucleate within the NC and UFG layers and on the boundary between layers of coarse and ultra-fine grained material. These local damages lead to meso-

cracks formation. Cracks are oriented not only across, but also along the direction of tension of a plate. Meandering cracks formed in the layers where the non-homogeneous compressive residual stresses attended. Results of fracture simulation of thin aluminium and magnesium sheets with distribution of grain sizes in the surface layers agree with experimental data. Figure 5b shows the structure of the cross-sectional specimen of Al-0.6% Mg-0.4% Si alloy after 47 cycles of tension and compression. The thickness of specimen was equal to 1.5 mm. The UFG layers have been created by the ultrasonic peening on the both surfaces of specimen. The parts of specimen have been cut into sections after testing. The cross section was done at the distance of ~ 2 mm from surface of fracture. In the section of the specimen observed microcracks oriented along the direction of the sample. Surface cracks are parallel to the plane of the sheet at different distances. The first system of cracks was formed in the interface region between UFG and CG material as predicted the results of simulation. The second system of cracks is formed in the zone of maximum gradient of residual stress. Micro-voids were created in the NC layers.

Fracture is a result of stochastic damage nucleation and growth. Structure heterogeneity may influence the random distribution of total plastic work over the model elementary volume. Therefore, fracture of fine-grained layer alloys with a bimodal grain size distribution under dynamic tension has probabilistic character.

The probability of microcracks nucleation within the material particles in layer with a grain size distribution can be described by the Eq. [18]:

$$P_r(W^p) = 1 - \exp[(\frac{W^p - W^p_{\min}}{W^p_0})^{\alpha}],\ W^p \geq W^p_{\min}, \tag{16}$$

where P_r is the Weibull probability function, $W_{p\,min}$ is the minimal possible total plastic work per unit volume at microscale level, α and W_{p0} are constant parameters of the distribution.

The damaged volume retains the resistance to plastic deformation during dynamic loading. Note that for the light alloys with bimodal grain size distributions, the ultrafine-grained volume can be considered as a quasi-brittle phase, in which the microcracks are generated during the plastic deformation while the macroscopic mechanical behavior exhibit good ductility. Thus, density of microcracks in the surface layer with grain size distribution can be written by Eq. (17) which is similar to Eq. referenced in [19]:

$$N = N_0 P_r(W^p) = N_0 \{1 - \exp[(\frac{W^p - W^p_{\min}}{W^p_0})^{\alpha}]\},\ W^p \geq W^p_{\min}, \tag{17}$$

where N is the density of microcracks, N_0 is the saturation density of microcracks at formation of mesoscopic crack.

Mesocracks nucleated within the UFG volume and propagates through the coarse grained volume. The strain to fracture of thin metal sheets with UFG layers was calculated as average strain at which cracks cross the elementary volume.

Figure 6 shows the calculated strain to fracture versus thickness of aluminum, magnesium and alpha-titanium sheets with surface UFG layers. Values of ε_f at tension were calculated at room temperature and strain rates ~ 1 s^{-1}.

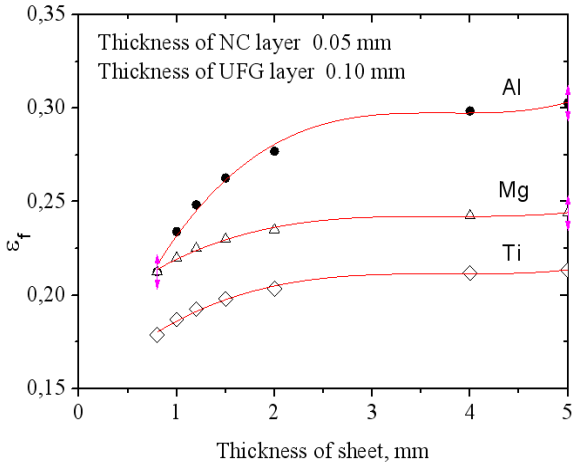

Figure 6. The strain to fracture vs thickness of aluminium, magnesium and titanium sheets.

The influence of surface nanostructured layers on the strain to fracture decreases with increasing thickness of the sheets. Since the thickness of the structured surface layers does not exceed 0.02-0.025 mm, the influence of layers on the resistance to plastic flow and the strain to fracture of metal sheet becomes insignificant when the thickness of the sheet more ~2.5 mm.

4 CONCLUSIONS

The multiscale computer simulation was used for the simulation of fracture of thin sheet of light alloys with distribution of grain sizes in the surface layers.

Fracture of fine-grained alloys under dynamic loading has probabilistic character and depends on parameters of structure heterogeneity. Formation of macro-scale failure zone is a result of several processes of structure evolution including damage nucleation, damage growth, and coalescence of damages. Damage nucleation is associated with strain localization at mesoscale level. Results of computer simulation demonstrate that the high strain localization in UFG alloys under dynamic loadings depends on the ratio between volume concentrations of fine and coarse grains. Fine precipitates in alloys not only affect the hardening but also lead to change the influence of the grains size distribution on volume concentration of shear bands. The dynamic ductility of UFG light alloys is increased when specific volume of coarse grains is greater than 30 %. Results of computer simulation can be used for estimation of grains size distribution influence on the dynamic strength and ductility of UFG alloys processed by severe plastic deformation methods.

ACKNOWLEDGMENT

This work was supported partially by the Grant from the President of Russian Federation, and by a grant from the Foundation of D. I. Mendeleev's National Tomsk State University within the Program of increasing the competitiveness of TSU. The authors are grateful for the support of this research.

REFERENCES

[1] S.O. Gashti, A. Fattah-alhosseini, Y. Mazaheri, M.K. Keshavarz, Effects of grain size and dislocation density on strain hardening behavior of ultrafine grained AA1050 processed by accumulative roll bonding. *Journal of Alloys and Compounds*, **658**, 854e861, 2016.

[2] X. Wu, N. Tao, Y. Hong et al. Microstructure and evolution of mechanically-induced ultrafine grain in surface layer of AL-alloy subjected to USSP. *Acta Materialia*, **50**, 2075–2084, 2002.

[3] Y. Huang, L. Wan, S. Lv, et al. Gradient micro-structured surface layer on aluminum alloy fabricated by in situ rolling friction stir welding. *Materials and Design.* **52**, 821–827, 2013.

[4] Y. Yin, W. Xu, Q. Sun, L. Xiao, J. Sun, Deformation and fracture behavior of commercially pure titanium with gradient nano-to-micron-grained surface layer. *Transaction Nonferrous Metal Society of China*, **25**, 738−747, 2015.

[5] G. Liu, S.C. Wang, X.F. Lou, J. Lu and K. Lu. Low carbon steel with nanostructured surface layer induced by high-energy shot peening. *Scripta materialia*, 44, 1791–1795, 2001.

[6] Yang, D.K. and Hodgson, P.D., Tough ultrafine-grained Ti through multilayering and grading, Scripta materialia, 68, 309–312, 2013.

[7] X. Guo, A.Y.T. Leung, A.Y. Chen, H.H. Ruan, J. Lu Investigation of non-local cracking in layered stainless steel with nanostructured interface. Scripta Materialia, 63, 403-406, 2010.

[8] J. Zhang, X. Ou, Thermal stability of nanocrystalline in surface layer of magnesium alloy AZ91D. Transaction Nonferrous Metal Society of China, 20, 1340−1344, 2010.

[9] R.K. Nalla, I. Altenberger, U. Noster et al. On the influence of mechanical surface treatments/deep rolling and laser shock peening/on the fatigue behavior of Ti64. *Materials Science and Engineering* , **A355**, 216–230, 2003.

[10] Wen M., Liu G., Gu J., et al. Dislocation evolution in titanium during surface severe plastic deformation. *Applied Surface Science*, **255,** 6097–6102, 2009.

[11] H.Q. Sun, Y.N. Shi, M.-X. Zhang, K. Lu. Surface alloying of an Mg alloy subjected to surface mechanical attrition treatment. *Surface and Coatings Technology*, **202**, 3947-3953, 2008.

[12] K. Lu, J. Lu Nanostructured surface layer on metallic materials induced by surface mechanical attrition treatment. *Materials Science and Engineering*, A **375-377**, 38-45, 2004.

[13] Y. Wei, B. Liu, L. Hou, et al. Characterization and properties of nanocrystalline surface layer in Mg alloy induced by surface mechanical attrition treatment. *Journal of Alloys and Compounds*, **452,** 336-342, 2008.

[14] X. Liao and Y. Zhao Surface. Nanocrystallization by surface mechanical attrition treatment. *Materials science forum*, **579**, 91-108, 2008.

[15] N. S. Prabhu, J. Joseyphus, T. S. N. Sankaranarayanan, B. R. Kumar Residual stress analysis in surface mechanical attrition treated (SMAT) iron and steel component materials by magnetic barkhausen emission technique, *IEEE Transactions on Magnetics*, 48, 4713 – 4717, 2012.

[16] K.Y. Luo, J.Z. Lu, Q.W. Wang, et al. Residual stress distribution of Ti-6Al-4V alloy under different ns-LSP processing parameters. *Applied Surface Science*, **285, B**, 607, 2013.

[17] M. Korzynski, T. Zarski, K. Korzynska Surface layer condition and the fatigue strength of an AZ91 alloy after ball peening. *Journal of Materials Processing Technology*, **211,** 1982–1988, 2011.

[18] Vinogradov, V., Hashin Z. Probabilistic energy based model for prediction of transverse cracking in cross-ply laminates. Int. J. of Solids and Structures. **42**, 365–392, 2005.

[19] L. Zhu, S. Shi, K. Lu, and J. Lu, A statistical model for predicting the mechanical properties of nanostructured metals with bimodal grain size distribution, *Acta Materialia*, **60**, 5762–5772, 2012.

[20] V.A. Skripnyak, N.V. Skripnyak, E.G. Skripnyak. Mechanical behavior of light alloys with bimodal grain size distribution. *Applied Mechanics and Materials*, **756**, 205-213, 2015.

[21] V.A. Skripnyak Mechanical behavior of nanostructured and ultrafine-grained materials under shock wave loadings. Experimental data and results of computer simulation, *Shock Compression of Condensed Matter-2012*, AIP Conference Proceedings 1426 , AIP, Melville, NY, 2012, 965-970.

[22] V.A. Skripnyak, E.G. Skripnyak, N.V. Skripnyak, et al. Failure mechanisms of light alloys with a bimodal grain size distribution. *11th. World Congress on Computational Mechanics (WCCM XI)*, Barcelona, Spain, 25-29 June, 2014. Vol. IV. P. 3915-3925.

[23] A. N. Parshikov, S.A. Medin. Smoothed particle hydrodynamics using interparticle contact algorithms. *Journal Computation Physics*, **180**, 358-382, 2002.

[24] K. E. Prasad, B. Li, N. Dixit, et al. The dynamic flow and failure behavior of magnesium and Magnesium Alloys. *JOM*, **66**, (2), 291-304, 2014.

[25] J. Li, F. Li, J. Cai et al. Comparative investigation on the modified Zerilli–Armstrong model and Arrhenius-type model to predict the elevated-temperature flow behaviour of 7050 aluminium alloy. *Computational Materials Science*, **71**, 56–65,2013.

[26] M.A. Meyers, A. Mishra, D.J. Benson, Mechanical properties of nanocrystalline materials. *Progress in Materials Science*, **51**, 427–556, 2006.

[27] T. Mukai, and K. Higashi. Ductility enhancement of ultra fine-grained aluminum under dynamic loadings. *Scripta materialia*, **44**, 1493–1496, 2001.

[28] H.J. Choi, , et. al., Deformation behavior of magnesium in the grain size spectrum from nano- to micrometer. *Material Science Engineering*, **A 527**, 1565–1570, 2010.

[29] N. Ono, R. Nowak, S. Miura. Effect of deformation temperature on Hall–Petch relationship registered for polycrystalline magnesium. *Materials Letters*, **58**, 39– 43, 2003.

[30] L.W. Mayer, M. Hackauf, l. Kruger, I. Shneider Compressive behavior of ultrafine-grained AA6063T6 over a wide range of strains and strain rates. *International Journal of Material Research*, **98**, (3), 1-9, 2007.

[31] S. Zherebtsov, E. Kudryavtsev, S. Kostjuchenko et al. Strength and ductility-related properties of ultrafine grained two-phase titanium alloy produced by warm multiaxial forging. *Materials Science and Engineering*, **A 536**, 190–196, 2012.